Single-step design of hydrogel-based microfluidic assays for rapid diagnostics

Dietmar Puchberger-Enengl,*[ab] Christian Krutzler,[c] Franz Keplinger,[a] and Michael J. Vellekoop[b]

For the first time we demonstrate a microfluidic platform for the preparation of biosensing hydrogels by in-situ polymerization of polyethyleneglycol diacrylate (PEG-DA) in a single step. Capillary pressure barriers enable the precise formation of gel microstructures for fast molecule diffusion. Parallel arrangement of these finger structures allows for macroscopic and standard equipment readout methods. The analyte automatically fills the space inbetween the gel fingers by the hydrophilic nature of the gel. Introducing the functional structures in the chip fabrication allows for rapid assay customization by making surface treatment, gel curing mask alignment and washing steps obsolete. Simple handling and functionality are illustrated by assays for matrix metalloproteinase, an important factor in chronic wound healing. Assays for total protein concentration and cell counts are presented, demonstrating the possibilities for a wide range of fast and simple diagnostics.

1 Introduction

For the success of microfluidic devices in point-of-care diagnostics, easy handling and fast operation are key points[1,2]. Incorporation of hydrogels in microfluidic chips has been shown to enable simple, parallel and sensitive biosensing. Sensors for measurements of glucose[3–5], phenol[6], organophosphates[7] and urea[8] have been presented. Hydrogels are a suitable matrix to store reagents[9,10], proteins[6,7,11,12], DNA[13], and cells[14–19] on microchips without loss of activity. In contrast to paper-based microfluidics, which has been investigated for mainly colorimetric ready-to-use diagnostic devices[20,21], hydrogel chips offer more flexibility for complex samples such as cell suspensions and for sensitive optical detection methods. Unlike sensors, based on surface immobilization a hydrogel contains the sensing reagent in a three-dimensional matrix and allows diffusion of the analyte through the pores of the gel. The diffusion time of reagents t is determined by

$$t \propto \frac{l^2}{D} \tag{1}$$

where l is the diffusion length and D the diffusion coefficient of the molecule of interest. Since the diffusion length l is determined by the size of the hydrogel structures, their dimensions have to be relatively small i.e. in the micrometer range to enable reactions within a reasonable short time. Furthermore, the pore size of the gel has to be large enough to facilitate diffusion.

In situ polymerization of gel particles within a microfluidic chip has been the preferred fabrication method. An advantage of this procedure over conventional bead assays is that an exact number of particles or amount of reagent can be placed in a chip. Photosensitive polyethlyeneglycol diacrylate (PEG-DA) has found broad application as a biocompatible hydrogel in tissue engineering[22,23] and allows photostructuring as well as pore size tuning over a wide range. Pore sizes of PEG-based hydrogels can be tuned by varying the molecular weight and concentration of the PEG-DA precursor. If pore sizes of up to micrometers are required, polyethyleneglycol in different molecular weights can be added as a porogen[24]. These tuning opportunities allow immobilization and handling of a wide range of species from small molecules up to cells. PEG-DA microgel structures have to be fabricated by UV exposure through a mask[4,5,18,25] or stepwise by a focused beam[26–29]. Another fabrication method for hydrogel assays is the prefabrication of gel beads by a droplet generator[3,14,30–32]. However, all these methods have in common that they require a subsequent washing step to remove unreacted precursor. Furthermore, in-situ gel assays need an additional surface modification step to improve gel adhesion to the chip[5–10,13,16,17]. The elaborate preparations and need for external operation compromise the usability of such microfluidic diagnostic tools.

In this contribution we present a microfluidic platform, which allows in-situ polymerization of hydrogel microstructures in

† Electronic Supplementary Information (ESI) available: Details of design considerations: Contact angle measurements, Illustration of chip geometry influence on the reaction. Full video of gel preparation and reaction according to Fig.2. See DOI: 10.1039/C3LC50944C

[a] *Institute of Sensor and Actuator Systems, Vienna University of Technology, 1040 Vienna, Austria. E-mail: dietmar.puchberger-enengl@tuwien.ac.at; Fax: +43-1-58801-36699; Tel: +43-1-58801-76675*

[b] *Institute for Microsensors, -actuators and -systems (IMSAS), MCB, University of Bremen, 28359 Bremen, Germany.*

[c] *Integrated Microsystems Austria GmbH, 2700 Wiener Neustadt, Austria*

a single step without surface modification and washing steps. Furthermore, no external operation is required to initiate a reaction. The first reagent is mixed with a gel precursor and introduced into the chip only in predefined regions. The regions of the gel micropattern and analyte are defined by capillary pressure barriers within the chip. An advancing fluid meniscus is pinned to a barrier and advances along it instead of crossing it. This concept of laplace pressure barriers has been presented earlier for controlled priming[33,34], valving[35] and pressure driven batch mixing[36,37].

A promising application is the assessment of impaired healing wounds, as they pose a major impact for patients and the health care system[38]. Healing mechanisms are very complex and wound status cannot be determined by a single marker but rather by a set of markers and diagnostic tools[39]. Markers under investigation include proteinase activity, protein concentration and the bacterial load of the wound. Elevated proteinase activity in wound fluids has been shown to correspond to delayed healing.[40–42] Literature values of relevant markers are summarized in table 1. The inability of clinicians to measure these markers in an efficient manner has prevented wound care to keep pace with scientific results. Therefore, quantitative and parallel diagnostics at the point-of-care would be an important tool to guide and evaluate clinical treatment of chronic wounds[43].

The functionality of the preseted microfluidic device is demonstrated by assays of matrix metalloproteinase 9 (MMP-9), protein concentration and cell counts.

Table 1 Literature values of biomarkers for wound assessment

Marker	healing (non-infected)	non-healing (infected)
Collagenases $(\mu g/ml)$[44]	0.76	22.8
active MMP-9 $(\mu g/ml)$[40]	1.18 ± 1.21	2.9 ± 1.64
Lysozyme $(\mu g/ml)$[45]	1.79 ± 1.22	24.2 ± 9.2
Total protein (mg/ml)[46]	44.3 ± 8.8	30 ± 7.6
Albumin (mg/ml)[46]	25 ± 2.3	17 ± 4.3
Glucose (mM)[47]	$5 - 7.6$	$0.3 - 1$
Bacteria counts (CFU/ml)[48,49]	$< 10^6$	$> 10^6$

2 Experimental

2.1 Chip Design and Operation Principle

The principle of the device is illustrated in Fig. 1. An advancing fluid meniscus is pinned to a capillary pressure barrier and propagates along it instead of crossing it (Fig. 1b). Therefore, liquid occupies only regions that are defined by the barriers within the chip. The liquid guiding effect of the fabricated

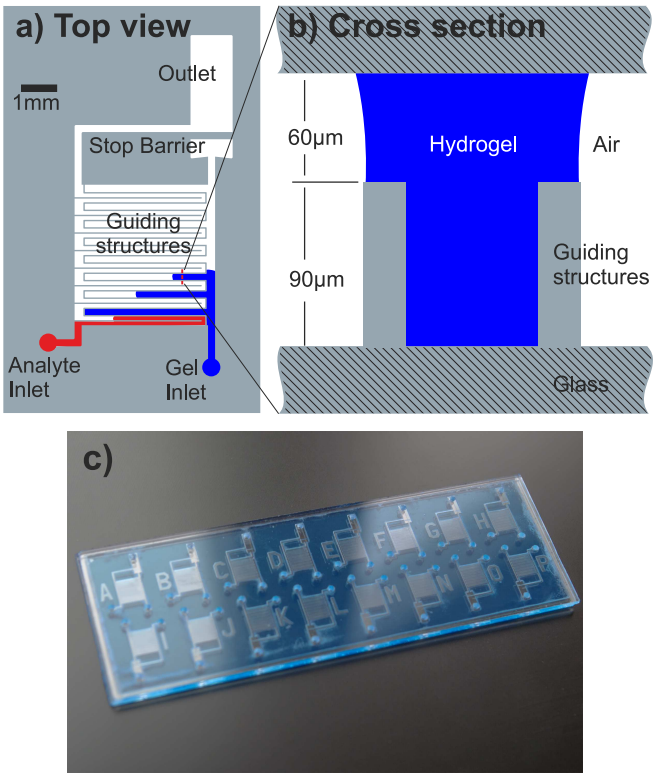

Fig. 1 Illustration of chip design. a) Top view: The device is prepared by injecting the sensing hydrogel via one inlet (blue). After curing, the analyte fills the chamber interdigitated to the gel and void-free (red). b) Cross section: Capillary pressure barriers enable reliable liquid guiding. c) Assembled device with 16 reaction chambers (microscope slide format). Dry film resist is sandwiched inbetween glass slides.

structures depends on the wetting properties of the gel precursor, the step height of the structures, and the gel interface on top of the structures. According to equation (1), the reaction speed depends on the width of the gel structures (see also Fig. S2†). As the contact angle difference between glass and the photoresist decreases with increasing polymeric precursor concentration, the step height has to be increased to enable reliable guiding. In practice, a step height larger than 60 % of the chamber height has shown robust guiding for the tested precursor solutions. Contact angle measurements in dependence on precursor concentrations are available as supplemental information (table S1†). The remaining gel interface height on top of the structures has only minor influence on the assay speed (Fig. S3†). However, the maximum is determined by the lateral gel dimensions (feature size), which on the other hand depends on the aspect ratio of the used resist material (Fig. S4†). The dimensions of the reaction chamber of $4\,mm$ x $4\,mm$ with $90\,\mu m$ high guiding structures and $60\,\mu m$ gel interface have shown to be a reliable trade-off of the mentioned

aspects. After injection and UV curing of the sensing hydrogel, the analyte fills the chamber interdigitated to the gel micro structures by capillary action (Fig. 1a).

Microfluidic chips are fabricated on a microscope glass slide ($76\,mm$ x $26\,mm$) by hot roll lamination of dry film photoresist, which allows fast, cost efficient and parallel processing. 16 devices are fabricated on a slide in a size and distance according to a 96 well plate in order to be compatible with standard fluorescence reader equipment. In a first fabrication step a layer of $90\,\mu m$ dry film resist (Ordyl SY300, Elga Europe) is laminated onto the bottom glass slide. The microfluidic chambers and pressure barriers are structured by standard photolithography. Inlet and outlet holes are powder-blasted into the top glass layer. Afterwards a $60\,\mu m$ dry film layer is laminated and structured onto the top glass. Both glass slides are aligned by eye and the two resist surfaces are bonded by hot roll lamination. An assembled device is shown in Fig. 1c.

2.2 Sensing Hydrogels, Samples and Experiments

The hydrogel consists of polyethyleneglycol diacrylate (PEG-DA) with a 2-hydroxy-2-methylpropiophenone (HMPP) photoinitiator. For the proteinase assays the hydrogel precursor is prepared by dissolving PEG-DA with a molecular weight of 6000 in Tris-HCl buffer ($pH7.6$) at $10\%w/v$. The HMPP photoinitiator is added at a concentration of $1.5\%v/v$. An autoquenching fluorescein conjugate proteinase substrate (DQ Gelatin, Invitrogen) is mixed with the gel precursor. Upon cleavage of the substrate by the proteinase, fluorescence intensity, corresponding to the enzyme activity can be measured.
Colorimetric protein detection is achieved by a color shift of bromophenol blue upon interaction with protein in an acidic environment.[50] Stock solutions for the colorimetric protein assay are prepared as follows: A) PEG-DA, molecular weight 700 mixed with $2\%v/v$ HMPP. B) Bromophenol blue in deionized water at $10\,mg/ml$. C) Polyethylenegylcol (PEG), MW 8000 in deionized water $50\%w/w$. The gel is mixed in ratios 1:2:1 (A:B:C).
Fluorescent protein assay gels are prepared by mixing $20\%w/v$ PEG-DA 6000, $1.5\%v/v$ HMPP and $5\%v/v$ of a protein specific dye (Qubit, Invitrogen) in the provided buffer. Gel for cell counts consists of $5\mu M$ Syto-9 in $20\%w/v$ PEG-DA 6000, $1.5\%v/v$ HMPP in Tris-HCl buffer. Blood samples were obtained from healthy volunteers, recruited at the Austrian Institute of Technology with informed consent. All experiments were performed in compliance with the relevant laws and institutional guidelines of the Austrian Institute of Technology, approved by the ethics board of the City of Vienna, Austria.
After introduction of the gel into the chip, it is cured by flood exposure at $365\,nm$ in a UV nail dryer for $30\,s$. The chips are sealed with tape and stored cool and dark until use. Samples for standard curves are prepared by serial dilutions of *Clostridium histolyticum* collagenase type IV (MMP-9) and bovine serum albumin. Cochineal red has been obtained from a local pharmacy, all other chemicals are ordered from Sigma Aldrich unless other mentioned. Fluorescence detection is done by a camera mounted on a Nikon Eclipse 80i fluorescence microscope with a B-2A filter set. In addition readings with a fluorescence spectrometer (Perkin Elmer LS55) are conducted.

3 Results and Discussion

After preparation of the chip for the desired assay, the reaction is initiated by adding a drop of the sample to the analyte inlet (Fig. 1a). The chip concept enables reactions with a minimum of reagent and sample volume per test. In contrast to conventional assays, only $1.5\,\mu l$ of sample are required. Reaction dynamics are illustrated in Fig.2*. The device in Fig.2a is prepared with a pH sensitive dye (bromophenol blue) incorporated in the hydrogel. Bromophenol blue exhibits a shift from blue to yellow at a pH value below 3. Citric acid (pH 2) with cochineal red (a red food dye) with a molecular weight of 604 is added to the chip to start the reaction (Fig.2c). Due to the hydrophilic nature of the gel the device fills completely automatic and void-free by capillary action. The fast response of bromophenol blue to the acidic environment is visible in Fig.2d. On the other hand, diffusion of the cochineal red molecules into the gel structures takes a bit longer. As seen in the picture Fig.2e, which was taken 2 min after the start of the experiment, the red dye has diffused into the hydrogel fingers. This result shows the dependencies of reaction dynamics on the molecule size and gel porosity. To yield assays with reasonable short response times (e.g. minutes), the gel composition has to be adjusted to the sample. By varying the molecular weight of the PEG-DA precursor or addition of a polyethyleneglycol diacrylate porogen the pore size and hence diffusion dynamics can be customized.
The pressure barrier height of $90\,\mu m$ ensures reliable guiding of liquids with different wetting properties due to varying content of monomers or solvents. Since the gel microstructures occupy about half the active chip area, the device is compatible with macroscopic readout equipment such as digital cameras, photodiodes or plate readers.

The functionality of the microfluidic chips for diagnostic applications is presented by assaying matrix metalloproteinase 9. Depending on the enzyme activity the collagene substrate in the hydrogel is cleaved and a green fluorescence signal is emitted (inset Fig. 3a). Results of three independent experiments are plotted in Fig.3a. Mean values and standard devi-

* Real time and uncut video of preparation and reaction is avialable as supplementary information.

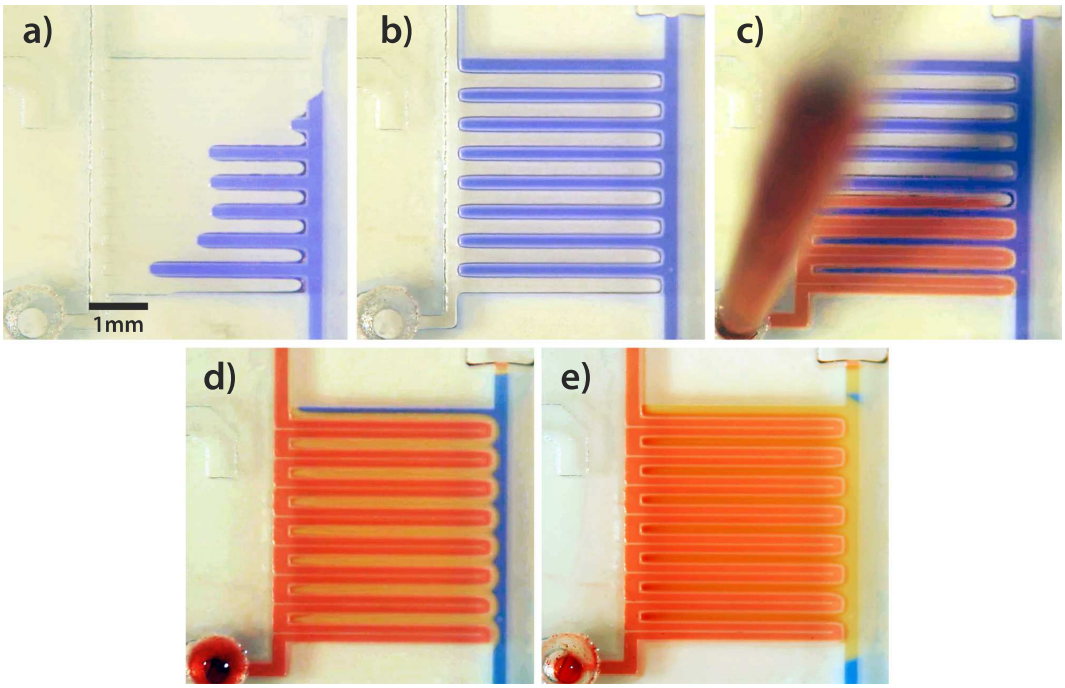

Fig. 2 Visualization of an assay reaction. a) Only $1\,\mu l$ of the the sensing hydrogel is required to prepare the chip. b) Device is ready for the assay with bromophenol blue pH indicator dye, immobilized in the UV cured hydrogel. c) Citric acid (pH 2) colored with cochineal red is topping up the chip interdigitated to the gel in order to have short diffusion paths. d) Fast (around $3\,s$) shift from blue to yellow of the pH indicator dye. e) Diffusion of the cochineal red dye into the hydrogel takes some time due to its molecular weight (MW 604). Picture taken after $120\,s$).

ation of image histograms are shown. As seen from the plot the sensitivity of the assay increases with incubation time. For concentrations in the range of $10\mu g/ml$ an incubation time of only 15 min is sufficient. With increasing incubation time, the limit of detection can be further decreased. Following the guidelines of the Clinical and Laboratory Standards Institute[51] a rough estimation of the limit of detection at an incubation time of $60\,min$ gives

$$L_D = \frac{mean_{blank} + 1.645\sigma_{blank} + 1.645\sigma_{lowC}}{sensitivity} = 0.47\mu g/ml \quad (2)$$

which is well below the values given in table 1. Readings with a fluorescence plate reader are shown in Fig.3b to demonstrate compatibility with standard laboratory equipment. As seen, results are in good agreement with image analysis.

Comparison of fluorescent and colorimetric total protein concentration measurements are summarized in Fig.4. Serial dilutions of bovine serum albumin are used for calibration. Incubation time after sample introduction was $10\,min$. The sensitivity of the fluorescent assay (Fig.4a) is much higher as for the colorimetric method, with a corresponding L_D of $0.02\,mg/ml$. On the other hand, colorimetric analysis are simply done by evaluating histogram values of the digital photograph. As seen from the inset in Fig.4b, the blue color intensity increases with increasing protein concentration. Limit of detection in this case calculates to $0.14\,mg/ml$, which still is well below the concentrations found in wound fluid samples (compare table 1).

The device is capable to handle complex samples as shown by an experiment with whole blood, collected by a finger prick from a healthy volunteer (Fig. 5). $2\,\mu l$ are collected and serially diluted 3 and 12 times, respectively. Syto-9, a cell permeable DNA fluorescent dye is incorporated into the gel. After an incubation time of $15\,min$ white blood cells are labeled green fluorescent. As mature red blood cells do not contain a nucleus and DNA the white blood cells are brightly visible. Counting the number of white blood cells has diagnostic applications in diseases such as leukemia[52], coronary heart disease[53], and systemic infection diagnostics. Furthermore, cell counts in wound fluid could be of additional value as excessive neutrophil invasion corresponds with wound severity[54]. Wound fluid analysis by performing the three presented fluorescent assays on a chip could give clinicians a quick and robust tool for estimation of chronic wound status. All three assays can be performed on the same chip with equal fluorescent detection (filter set 450-490/500/515).

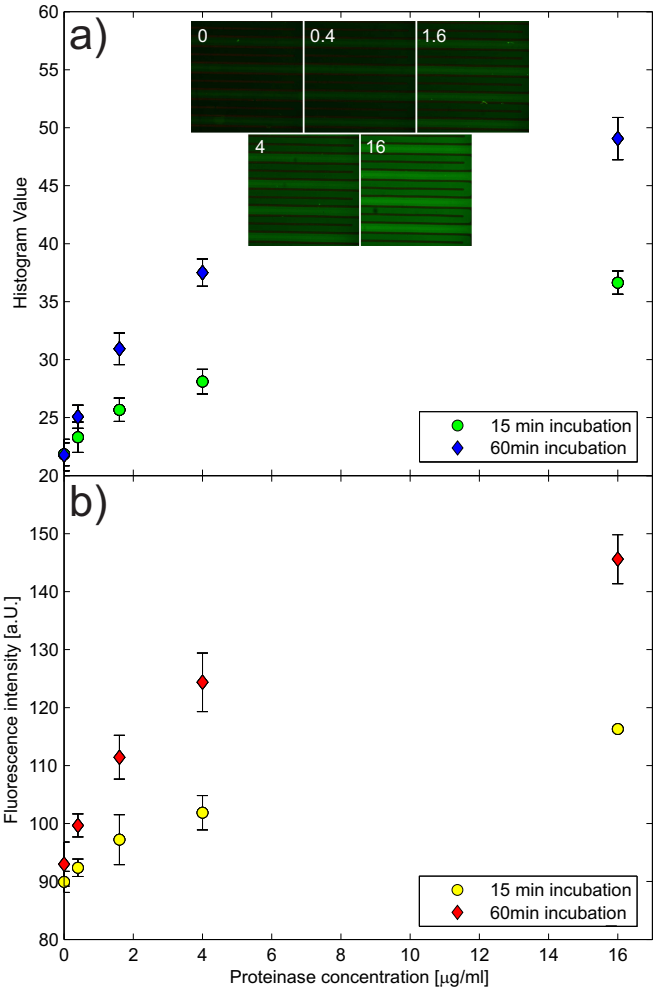

Fig. 3 Data evaluation of fluorescent images of the metalloproteinase assay. Mean histogram values are plotted versus enzyme activity of MMP-9. a) Results of 3 consecutive experiments are summarized. Data shows results after 15 min and 60 min incubation, respectively. b) Readings of a fluorescence plate reader are in good agreement with image analysis. (excitation 490 nm, slit 5, emission 525 nm slit 10, 515 nm cut-off)

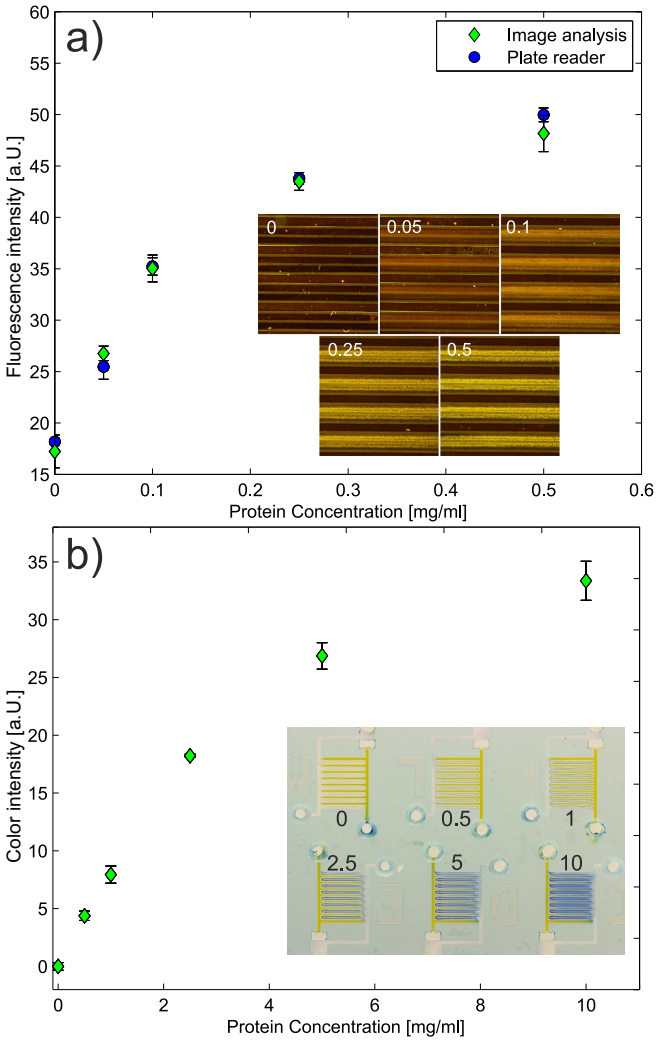

Fig. 4 Total protein concentration assays. a) Fluorescent protein assay results from image analysis and plate reader (excitation 490 nm, slit 5, emission 560 nm slit 20, 515nm cut-off). b) Colorimetric protein assay. Bromophenol blue exhibits a color shift from yellow to blue in an acidic environment upon addition of protein. All experiments conducted in triplets, readings are done after 10 min of incubation time.

4 Conclusions

In this contribution we have demonstrated a method for the rapid preparation of hydrogel-based bioassays in a single step. The simple handling and operation allows the end user to customize the microfluidic chip for different biosensing applications. As the chip dimensions define the reaction volume, pipetting errors by the user can be excluded. Compatibility with standard equipment has been proven, which is an important step towards clinical acceptance.

By the simple dry film process the chips can be produced by any standard facility. Future large scale production could also be achieved by hot embossing methods, as the guiding effect does not necessitate different wetting properties.

The presented enzyme, protein and cell assays indicate the vast amount of possibilities for biochemical testing. Hydrogel-based assays are especially suitable for enzyme activity, enzymatic sensing and direct target labeling assays, allowing for instantaneous readout. However, hydrogels also support antibody binding within the three-dimensional matrix, with the specific advantages of maintaining excellent stability and yielding higher signals than planar assay due to higher

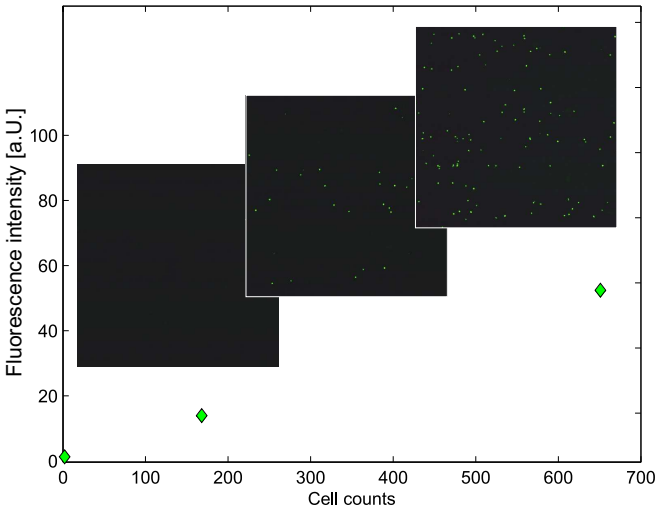

Fig. 5 Handling of complex samples: Fluorescent staining of white blood cells with Syto-9 in a blood sample. Fluorescence image intensity is plotted against an automated cell count. From left to right: Negative control, 12-fold and 3-fold dilution of a drop of whole blood.

loading[14,55]. Performing homogeneous immunoassays would enable detection of specific rare protein markers in the same rapid manner as the presented assays[56]. We strongly believe that the evolution of user friendly microfluidics will yield analytical tools in clinical applications. Combining several analytical tests on a single slide offers the possibility to obtain multi-parametric analysis at the point-of-care. Such tests would help to investigate complex diseases such as chronic wound healing, where many factors contribute to stalled healing.

Acknowledgements

This work was part of the project *Multiparametric sensors for wound status characterization* of the *Austrian Comet Center for Medical Innovation and Technology*.

References

1 G. M. Whitesides, *Lab on a chip*, 2013, **13**, 11–3.
2 L. Gervais and E. Delamarche, *Lab on a chip*, 2009, **9**, 3330–3337.
3 C. Kantak, Q. Zhu, S. Beyer, T. Bansal and D. Trau, *Biomicrofluidics*, 2012, **6**, 22006–220069.
4 D. Choi, A. E. Jang, A. J. Park and W.-g. Koh, *Microfluid Nanofluid*, 2008, 703–710.
5 E. Jang, S. Kim and W.-G. Koh, *Biosensors & bioelectronics*, 2012, **31**, 529–36.
6 E. Jang, K. J. Son, B. Kim and W.-G. Koh, *The Analyst*, 2010, **135**, 2871–8.
7 V. K. Yadavalli, W.-G. Koh, G. J. Lazur and M. V. Pishko, *Sensors and Actuators B: Chemical*, 2004, **97**, 290–297.
8 W.-G. Koh and M. Pishko, *Sensors and Actuators B: Chemical*, 2005, **106**, 335–342.
9 L. Lin, Z. Gao, H. Wei, H. Li, F. Wang and J.-M. Lin, *Biomicrofluidics*, 2011, **5**, 034112.
10 N. Y. Lee, Y. K. Jung and H. G. Park, *Biochemical Engineering Journal*, 2006, **29**, 103–108.
11 Q. Wang, Z. Yang, L. Wang, M. Ma and B. Xu, *Chemical communications*, 2007, 1032–4.
12 V. Pedrosa, J. Yan, A. L. Simonian and A. Revzin, *Electroanalysis*, 2011, **23**, 1142–1149.
13 J. Liu, D. Gao, H.-F. Li and J.-M. Lin, *Lab on a chip*, 2009, **9**, 1301–5.
14 K. G. Lee, T. J. Park, S. Y. Soo, K. W. Wang, B. I. I. Kim, J. H. Park, C.-S. Lee, D. H. Kim and S. J. Lee, *Biotechnology and bioengineering*, 2010, **107**, 747–51.
15 W.-G. Koh, A. Revzin and M. V. Pishko, *Langmuir*, 2002, **18**, 2459–62.
16 D. Gao, J. Liu, H.-B. Wei, H.-F. Li, G.-S. Guo and J.-M. Lin, *Analytica chimica acta*, 2010, **665**, 7–14.
17 D. R. Albrecht, V. L. Tsang, R. L. Sah and S. N. Bhatia, *Lab on a chip*, 2005, **5**, 111–8.
18 J. Heo, K. J. Thomas, G. H. Seong and R. M. Crooks, *Analytical chemistry*, 2003, **75**, 22–6.
19 S. J. Trietsch, G. D. Israëls, J. Joore, T. Hankemeier and P. Vulto, *Lab on a chip*, 2013.
20 X. Li, D. R. Ballerini and W. Shen, *Biomicrofluidics*, 2012, **6**, 011301.
21 A. K. Yetisen, M. S. Akram and C. R. Lowe, *Lab on a chip*, 2013, **13**, 2210–51.
22 B. G. Chung, K.-H. Lee, A. Khademhosseini and S.-h. Lee, *Lab on a chip*, 2012, **12**, 45–59.
23 N. Annabi, J. W. Nichol, X. Zhong, C. Ji, S. Koshy, A. Khademhosseini and F. Dehghani, *Tissue engineering. Part B, Reviews*, 2010, **16**, 371–83.
24 A. G. Lee, C. P. Arena, D. J. Beebe and S. P. Palecek, *Biomacromolecules*, 2010, **11**, 3316–24.
25 H. M. Simms, C. M. Brotherton, B. T. Good, R. H. Davis, K. S. Anseth and C. N. Bowman, *Lab on a chip*, 2005, **5**, 151–7.
26 C. L. Lewis, Y. Lin, C. Yang, A. K. Manocchi, K. P. Yuet, P. S. Doyle and H. Yi, *Langmuir*, 2010, **26**, 13436–41.
27 L. N. Kim, S.-e. Choi, J. Kim, H. Kim and S. Kwon, *Lab on a chip*, 2011, **11**, 48–51.
28 S. E. Chung, W. Park, S. Shin, S. A. Lee and S. Kwon, *Nature materials*, 2008, **7**, 581–7.
29 D. C. Appleyard, S. C. Chapin, R. L. Srinivas and P. S. Doyle, *Nature protocols*, 2011, **6**, 1761–74.
30 W.-H. Tan and S. Takeuchi, *Advanced Materials*, 2007, **19**, 2696–2701.
31 R. F. Shepherd, J. C. Conrad, S. K. Rhodes, D. R. Link, M. Marquez, D. a. Weitz and J. a. Lewis, *Langmuir*, 2006, **22**, 8618–22.
32 C.-h. Choi, J.-h. Jung, T.-s. Hwang and C.-s. Lee, *Macromolecular Research*, 2009, **17**, 163–167.
33 D. Puchberger-Enengl, S. Podszun, H. Heinz, C. Hermann, P. Vulto and G. a. Urban, *Biomicrofluidics*, 2011, **5**, 044111.
34 P. Vulto, S. Podszun, P. Meyer, C. Hermann, A. Manz and G. a. Urban, *Lab on a chip*, 2011, **11**, 1596–602.
35 G. Takei, M. Nonogi, A. Hibara, T. Kitamori and H.-B. Kim, *Lab on a chip*, 2007, **7**, 596–602.
36 J. Melin, G. Gimenéz, N. Roxhed, W. van der Wijngaart and G. Stemme, *Lab on a chip*, 2004, **4**, 214–9.
37 S. Hakenberg, M. Hügle, M. Weidmann, F. Hufert, G. Dame and G. a. Urban, *Lab on a chip*, 2012, **12**, 4576–80.
38 C. K. Sen, G. M. Gordillo, S. Roy, R. Kirsner, L. Lambert, T. K. Hunt, F. Gottrup, G. C. Gurtner and M. T. Longaker, *Wound repair and regeneration*, 2009, **17**, 763–71.
39 World Union of Wound Healing Societies (WUWHS), *Principles of best practice: Diagnostics and wounds. A consensus document.*, Mep ltd tech-

nical report, 2008.
40 Y. Liu, D. Min, T. Bolton and V. Nubé, *Diabetes care*, 2009, **32**, 1734–1736.
41 M. J. Reiss, Y.-P. Han, E. Garcia, M. Goldberg, H. Yu and W. L. Garner, *Surgery*, 2010, **147**, 295–302.
42 E. Rayment, Z. Upton and G. K. Shooter, *The British journal of dermatology*, 2008, **158**, 951–61.
43 R. J. Snyder, B. Cullen and L. T. Nisbet, *International wound journal*, 2012, 1–10.
44 N. J. Trengove, M. C. Stacey, S. Macauley, N. Bennett, J. Gibson, F. Burslem, G. Murphy and G. Schultz, *Wound Repair and Regeneration*, 1999, **7**, 442–452.
45 A. Hasmann, E. Wehrschuetz-Sigl, G. Kanzler, U. Gewessler, E. Hulla, K. P. Schneider, B. Binder, M. Schintler and G. M. Guebitz, *Diagnostic microbiology and infectious disease*, 2011, **71**, 12–23.
46 T. J. James, M. a. Hughes, G. W. Cherry and R. P. Taylor, *Wound repair and regeneration*, 2000, **8**, 264–9.
47 S. Iizaka, H. Sanada, T. Minematsu, M. Oba, G. Nakagami, H. Koyanagi, T. Nagase, C. Konya and J. Sugama, *Wound repair and regeneration*, 2010, **18**, 31–7.
48 S. E. Gardner, R. a. Frantz, C. L. Saltzman, S. L. Hillis, H. Park and M. Scherubel, *Wound repair and regeneration*, 2006, **14**, 548–57.
49 L. Xu, S. V. McLennan, L. Lo, A. Natfaji, T. Bolton, Y. Liu, S. M. Twigg and D. K. Yue, *Diabetes care*, 2007, **30**, 378–80.
50 Y. J. Wei, K. a. Li and S. Y. Tong, *Talanta*, 1996, **43**, 1–10.
51 D. a. Armbruster and T. Pry, *The Clinical biochemist. Reviews / Australian Association of Clinical Biochemists*, 2008, **29 Suppl 1**, S49–52.
52 E. H. Estey, *American journal of hematology*, 2012, **87**, 89–99.
53 G. Twig, A. Afek, A. Shamiss, E. Derazne, D. Tzur, B. Gordon and A. Tirosh, *PloS one*, 2012, **7**, e47183.
54 R. F. Diegelmann, *Wound repair and regeneration*, 2003, **11**, 490–5.
55 Y. Lee, H. J. Lee, K. J. Son and W.-G. Koh, *Journal of Materials Chemistry*, 2011, **21**, 4476.
56 T. Kreisig, R. Hoffmann and T. Zuchner, *Analytical chemistry*, 2011, **83**, 4281–7.